Journal of Statistical Physics, Vol. 45, Nos. 5/6, 1986

Computational Study of Propagating Fronts in a Lattice-Gas Model

Alan R. Kerstein[1]

Received July 1, 1986; revision received August 26, 1986

Velocities and other features of propagating fronts in the lattice-gas model analyzed by Bramson *et al.* are computed by Monte Carlo simulation. The propagation velocity $v(\gamma)$ is found to converge slowly to its asymptotic dependence on the exchange-rate parameter γ. The number density of occupied sites in the "interaction zone" (extending from the forwardmost occupied to the rearmost unoccupied site) appears to converge to 2/3 for large γ. Spatial profiles of site occupancy and interface number density for finite γ are compared to the profiles originally computed by Fisher using the differential equation obeyed in the large-γ limit. Several significant features inferred from the computations have not yet been explained analytically.

KEY WORDS: Lattice gas; interacting particle system; velocity selection; diffusion-reaction equation.

1. INTRODUCTION

Lattice-gas models that obey diffusion-reaction equations in a hydrodynamic limit are useful for identifying selection mechanisms governing diffusion-reaction systems.[1] In some instances, the lattice-gas model may be of interest in its own right because it may represent physical phenomena not only in the hydrodynamic limit, but also away from the limit, where diffusion-reaction equations are not applicable. Such a model has been formulated and analyzed by this author with reference to turbulent flame propagation in fuel-air mixtures.[2]

A special case of the model has been analyzed by Bramson *et al.*[3] There it is shown that the velocity of a front propagating through the lattice gas obeys a selection principle that is consistent with the well-known

[1] Sandia National Laboratories Livermore, California 94550.

0022-4715/86/1200-0921$05.00/0

velocity-selection principle[4,5] governing the differential equation obtained in the hydrodynamic limit.

Here, some computational results are presented for the version of the model studied by Bramson *et al.*[3] The computations address the rate of convergence to the hydrodynamic limit and lattice-gas properties in that limit, some of which have no continuum analog. The results suggest some simple relationships that have not yet been obtained analytically.

2. MODEL FORMULATION AND MOTIVATION

The lattice-gas model, as formulated by Bramson *et al.*,[3] is briefly recapitulated. Sites labeled by integers $-\infty < i < +\infty$ are occupied or unoccupied, represented by values 1 and 0, respectively, of the state variable $\eta(i)$. The state may change due to either an exchange of state between a pair of adjacent sites (expressed by Bramson *et al.* as a particle jump) or a creation event. Each pair of adjacent sites exchanges states at a rate $\gamma/2$. Each unoccupied site i is changed to occupied (particle creation) at a rate $[\eta(i-1)+\eta(i+1)]/2$.

Starting, say, from the step-function initial condition $\eta = 0$ for positive i, otherwise $\eta = 1$, the propagation velocity v is defined as the long-time limit of the number of creation events per unit time. Several equivalent definitions have been identified,[3] as elaborated shortly. Defining the site occupancy as $u(i) = P[\eta(i) = 1]$ and rescaling length according to $x = i/\sqrt{\gamma}$, we find that in the hydrodynamic (large-γ) limit, $u(x, t)$ obeys the diffusion-reaction equation

$$\frac{\partial u}{\partial t} = \frac{1}{2}\frac{\partial^2 u}{\partial x^2} + u(1-u) \tag{1}$$

According to the selection principle[4,5] governing diffusion-reaction equations of this type [with mild regularity conditions imposed on $u(x, 0)$], $u(x, t)$ converges at large t to the traveling-wave form $u(x, t) = u(x - v_c t/\sqrt{\gamma})$ with propagation velocity

$$v_c = (2\gamma)^{1/2} \tag{2}$$

The subscript c denotes the velocity for the continuum model, Eq. (1), with velocity expressed in the unscaled coordinate i. This result also follows directly from analysis of the large-γ limit of the lattice-gas model.[3]

It is useful to define the number density of interfaces at i to be $f(i) = P[\eta(i) \neq \eta(i+1)]$. The expected total number of interfaces, i.e., sites with state different from the neighbor on the right, is $\langle F \rangle = \sum_{i=-\infty}^{\infty} f(i)$. Inter-

faces play a key role because all changes of the state variable occur at interfaces.

For finite γ, the lattice-gas propagation velocity not only departs from the form given by Eq. (2), but converges in the limit $\gamma \to 0$ to a distinct form,[2,3]

$$v = (1 + \gamma)/2 \tag{3}$$

Comparison of Eqs. (2) and (3) indicates that the transition between limits is nontrivial, and, in fact, no theory of this transition exists. Thus, the lattice-gas model raises significant mathematical questions not only in the hydrodynamic limit, but also in regimes that have no known continuum representation.

The transition between limits is also of physical interest with respect to the combustion application that originally motivated the model. In a turbulent, burning fuel–air mixture, two processes contribute to the time-evolving partition of the mixture into unburned and burned zones. First, turbulent convection stirs the mixture in a manner that can often be modeled adequately as a diffusion process.[6] In the lattice-gas model, the pair-exchange process induces a random walk of the particles with diffusivity $\gamma/2$, which is interpreted[2] as the turbulent diffusivity. Second, unburned mixture is converted to burned as the flame front penetrates the unburned zone, with a mass conversion rate per unit interfacial area which is taken, for modeling purposes, to be constant. In the lattice-gas model, flame front penetration is represented by the creation process, with the penetration rate normalized to 1/2. With this normalization, γ represents a ratio of turbulence intensity to flame front penetration rate. Experimentally accessible values of this ratio range from small values for which Eq. (3) is valid to large values for which Eq. (2) is valid. Computational results spanning this range of values have been found to be in agreement with the measured γ dependence of the burning rate of turbulent fuel–air mixtures.[2] (Note: In Ref. 2, γ is denoted as D.)

Alternative definitions of the propagation velocity are now introduced and interpreted physically in the context of the combustion application. The aforementioned definition, namely the rate of particle creation, corresponds to the total rate of mass conversion from unburned to burned. An alternative definition of the propagation velocity is

$$v \equiv \langle F \rangle / 2 \tag{4}$$

reflecting the fact that creation events occur with a rate 1/2 at each interface. Since the burning rate of the fuel–air mixture is the local penetration rate times the surface area of the interface ("flame front") separating the

burned and unburned zones, we infer that $\langle F \rangle$ is a representation of this interfacial area. More concretely, the lattice-gas model may be viewed as a discretized model of a line of sight through the fuel–air mixture, with $\langle F \rangle$ interpreted as the mean number of times the line intersects the highly convoluted flame front.

Another equivalent[3] definition employed here is

$$v \equiv \frac{1}{2} + \frac{\gamma}{2} P[\eta(i_r - 1) = 1] \tag{5}$$

where $i_r = \max\{i: \eta(i) = 1\}$. This definition has no obvious physical interpretation.

For analytical purposes, it has proven useful to choose a spatial coordinate moving with the front, e.g., by expressing site location as $i - i_r$. Computations are most conveniently performed with respect to the spatial coordinate $i - i_l + 1$, where $i_l = \min\{i: \eta(i) = 0\}$. Computational results characterizing the spatial structure of the propagating front are most conveniently interpreted using the coordinate $j = i - c$, where the "center of propagation" c is defined as the total number of creation events that have occurred. At any instant, the number of unoccupied sites in the interval $-\infty < j \leqslant 0$ is equal to the number of occupied sites in the interval $0 < j < \infty$, because exchange events change these quantities by equal amounts, while the changes induced by creation events are subsumed in the updating of c.

3. COMPUTATIONAL METHOD

Computations were performed using two different methods, so that the results could be verified by cross-checking. In the first method, the vector of state variables $\eta(i)$ is represented by a string of 0's and 1's, starting from the step-function initial condition specified earlier. Only the interval extending from the leftmost 0 to the rightmost 1 need be represented, since changes of state occur only at interfaces. (As such changes occur, the interval is updated as needed.) Assume that the interval contains n sites at some instant. An integer $0 \leqslant j \leqslant n$ is selected at random. If $\eta(j) \neq \eta(j+1)$, then sites j and $j+1$ undergo an exchange event with probability $\gamma/(\gamma+1)$, or a creation event with probability $1/(\gamma+1)$. [Recall that $\eta(0) = 1$ and $\eta(n+1) = 0$.] If the event changes the number F of interfaces, then F is updated. c is incremented by unity for each creation event.

In the second method, only a list of interfaces is stored in memory, so an integer $1 \leqslant j \leqslant F$ is randomly selected to determine the interface at which the next event occurs. In all other respects, the computation is

analogous to the first method. Though the difference between the methods may seem minor, the details of implementation are sufficiently disparate so that the two methods provide a cross-check of the results.

The first two definitions of v in Section 2 require estimates of c/t and $\langle F \rangle$, respectively, where t is the elapsed time and the brackets denote a time average. If the jth event leaves the system in a state with F_j interfaces, any of $2F_j$ events (an exchange or a creation at any of F_j interfaces) may occur next. The exchange rate is $\gamma/2$ per interface, while the creation rate is $1/2$ per interface, giving a next-event rate of $(\gamma+1)F_j/2$. The time interval τ_j until the next event is therefore exponentially distributed with mean $[(\gamma+1)F_j/2]^{-1}$. The elapsed time until the kth event is $t=\sum_{j=0}^{k-1}\tau_j$. An unbiased estimate of t is obtained by replacing τ_j by its mean value, giving

$$t=\sum_{j=0}^{k-1}\left[\frac{(\gamma+1)F_j}{2}\right]^{-1}=\frac{2}{\gamma+1}\sum_{j=0}^{k-1}F_j^{-1} \tag{6}$$

The advantage of this formulation is that the generation of random numbers to select values of the time intervals τ_j is avoided. Likewise, an unbiased estimate of the time average of any statistic A governing the system is obtained by replacing the definition $\langle A \rangle \equiv t^{-1}\sum_{j=0}^{k-1} A_j\tau_j$ by

$$\langle A \rangle = \sum_{j=0}^{k-1} A_j F_j^{-1} \Big/ \sum_{j=0}^{k-1} F_j^{-1} \tag{7}$$

where Eq. (6) has been used to estimate t. In particular, this gives

$$\langle F \rangle = k \Big/ \sum_{j=0}^{k-1} F_j^{-1} \tag{8}$$

These expressions are used to evaluate all time-averaged quantities discussed in the next section. However, statistics are not gathered during the period of transient relaxation from the initial step function. In each simulated realization, the number of events devoted to transient relaxation is equal to the number k of subsequent events for which statistics are gathered. k is deemed to be sufficiently large if velocity estimates based on k events and $k/10$ events, respectively, agree within statistical uncertainty, and if estimates for given k based on the different definitions of velocity likewise agree. In practice, the latter is found to be the more stringent criterion.

4. RESULTS AND DISCUSSION

Table I displays estimates of the propagation velocity and other quantities for γ values ranging from 10^{-1} to 10^3. Velocity estimates are divided

Table I. Velocity Estimates and Interaction-Zone Statistics for Computations with Indicated Values of the Exchange-Rate Parameter γ and the Number k of Events Contributing to the Estimate[a]

					Interaction zone		
γ	k	v_1/v_c	v_2/v_c	v_3/v_c	Number of 1's	Number of 0's	
0.1	10^4	1.222	1.228	1.226	0.076	0.051	(S)
		1.225	1.227	—	—	—	(I)
1	10^5	0.6343	0.6329	0.6368	0.745	0.470	(S)
		0.6343	0.6343	—	—	—	(I)
10	10^5	0.6137	0.6185	0.6187	6.28	3.61	(S)
		0.6020	0.5969	—	—	—	(I)
10	10^6	0.6197	0.6194	0.6183	6.33	3.60	(S)
		0.6157	0.6206	—	—	—	(I)
100	$10.^6$	0.7216	0.7281	0.7071	39.29	20.67	(S)
		0.7052	0.7117	—	—	—	(I)
100	5×10^6	0.7117	0.7085	0.7152	37.93	19.97	(S)
		0.7124	0.7137	—	—	—	(I)
1000	5×10^6	0.8320	0.8364	0.7010	186.05	102.80	(S)
	5×10^7	0.7992	0.7953	0.8184	187.30	92.90	(S)

[a] Results for three different definitions (see text) v_1, v_2, and v_3 of the propagation velocity are shown. (v_c is the propagation velocity in the continuum limit.) For the first two definitions, results are shown for interface-based (I) as well as site-based (S) computations. Also shown are the mean numbers of occupied sites (1's) and unoccupied sites (0's) in the interaction zone, extending from the forwardmost 1 to the rearmost 0.

by v_c, given by Eq. (2), in order to highlight the convergence to large-γ asymptotic behavior. The first velocity estimate is based on the particle-creation definition, $v_1 = c/t$. The second, "interface" definition v_2 is based on Eq. (4), with Eq. (8) used to estimate $\langle F \rangle$. The third definition v_3 is based on Eq. (5), where the indicated probability is computed by applying the time-averaging procedure of Eq. (7).

Estimates are shown from both the site-based (S) and the interface-based (I) computations, providing a cross-check as well as an indication of statistical uncertainty. For each $\gamma > 1$, results are shown for two values of k to provide an indication of transient effects. For $\gamma = 10$ and 100, only at the largest k value is the spread of the estimates v_1, v_2, and v_3 roughly the same as the spread between (S) and (I) estimates for a given definition of v. The

increase of relaxation time with increasing γ rendered computations for $\gamma \sim 10^4$ or larger intractable with the available computational resources.

The most noteworthy feature of the velocity estimates is the slow convergence to large-γ asymptotic behavior. For $\gamma \geqslant 10$, each decade increase in γ increases v/v_c by about 0.09, indicating a logarithmic dependence on γ. This slow convergence indicates the need for caution in applying asymptotic results such as Eq. (2) to experimental results obtained at finite γ.[2] In contrast, the convergence to the small-γ asymptotic behavior given by Eq. (3) is rapid. [Equations (2) and (3) predict $v/v_c = 1.230$ for $\gamma = 0.1$ and 0.707 for $\gamma = 1$.]

Other quantities displayed are the mean numbers of 1's and 0's, respectively, in the "interaction zone," extending from the forwardmost 1 (site i_r) to the rearmost 0 (site i_l). The results suggest that the number density of 1's in the interaction zone converges to 2/3 for large γ. This convergence appears to be more rapid than the velocity convergence. These observations have not yet been explained analytically.

The interaction zone and quantities characterizing it have no obvious continuum analogs, indicating that even in the hydrodynamic limit, the lattice gas may exhibit mathematically interesting properties that are not captured by the diffusion-reaction equation (1).

Another interesting feature with no continuum analog is the distribution of the number z of consecutive unoccupied sites immediately behind the forwardmost occupied site (site i_r). It has been conjectured[7] that for large γ, this distribution is approximately exponential in z, i.e., of the form

$$p(z) = (1 - e^{-\lambda}) e^{-\lambda z}, \qquad z = 0, 1, 2, \ldots \tag{9}$$

where the γ dependence of λ follows from comparison to Eqs. (2) and (5). Namely, $z = 0$ if and only if $\eta(i_r - 1) = 1$, so $p(0)$ can be substituted for $P[\eta(i_r - 1) = 1]$ in Eq. (5). In conjunction with Eq. (2), the large-γ limit gives

$$\lambda = (8/\gamma)^{1/2} \tag{10}$$

The slow convergence of v_3 to its asymptotic γ dependence, shown in Table I, indicates that the inferred γ dependence of λ will be exhibited only at γ values higher than those of Table I. However, the exponential dependence on z for given γ is obeyed at computationally accessible γ values, as illustrated by results for $\gamma = 100$ and $k = 5 \times 10^6$, shown in Fig. 1. The value of λ inferred from this computation is about one-third smaller than the value predicted by Eq. (10).

Finally, computed spatial profiles of site occupancy $\langle \eta(j) \rangle$ and interface number density $\langle f(j) \rangle$ are compared to profiles of their continuum

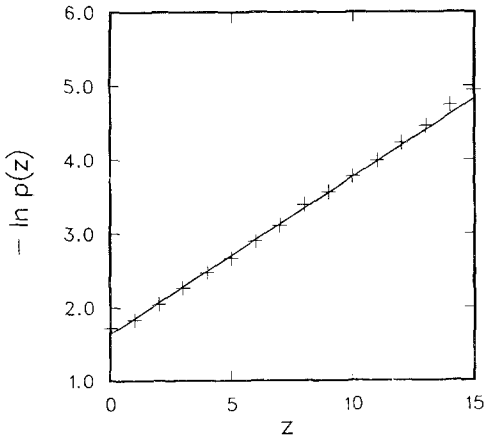

Fig. 1. Plot of $-\ln p(z)$ versus number z of consecutive unoccupied sites immediately behind the forwardmost occupied site, where $p(z)$ is the probability of z such sites, computed for $\gamma = 100$, $k = 5 \times 10^6$. The fitted line has slope 0.212, in contrast to the asymptotic prediction $\lambda = (8/\gamma)^{1/2} = 0.283$.

analogs. Figure 2 shows computed profiles of site occupancy for two γ values. The profiles are plotted with respect to the reduced coordinate $x = j/\sqrt{\gamma}$, where $j = i - c$, so that they are directly comparable to the continuum quantity $u(x)$, which is also shown. (Recall that c is the "center of propagation.") $u(x)$ is the numerically computed solution (originally obtained by Fisher[8]) of the equation

$$\frac{1}{2}\frac{\partial^2 u}{\partial x^2} + \sqrt{2}\frac{\partial u}{\partial x} + u(1-u) = 0 \tag{11}$$

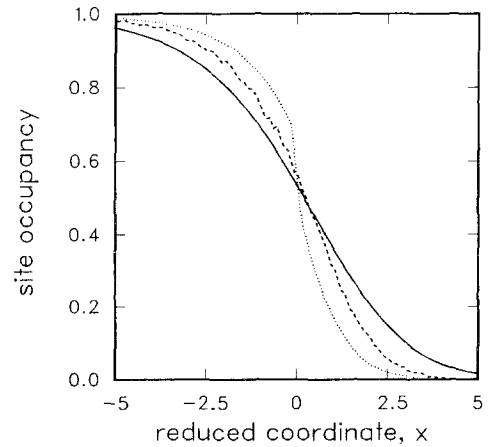

Fig. 2. Site occupancy versus reduced coordinate $x = j/\sqrt{\gamma}$ for (···) $\gamma = 10$ and (– –) $\gamma = 100$. (——) The continuum profile u, based on Eq. (11).

This equation for the steady-state profile $u(x)$ is obtained by substituting $u(x, t) = u(x - v_c t/\sqrt{\gamma})$, with $v_c = (2\gamma)^{1/2}$, into Eq. (1). Fisher provides a detailed discussion of the regularity conditions that determine the solution of Eq. (11), which corresponds to the steady-state profile obtained after relaxation, according to Eq. (1), from the initial step-function profile.

It is evident from Fig. 2 that convergence to the continuum profile is slow. This may be a reflection of the slow convergence of the propagation velocity to its continuum behavior. If the coordinate rescaling is expressed as $x = j\sqrt{2}/v_c$, then the effect of the slow convergence to v_c may be mitigated by choosing instead the reduced coordinate $x = j\sqrt{2}/v$, where v is a computed velocity estimate. In particular, defining $\hat{v} = v/v_c$, the results of Table I suggest values $\hat{v} = 0.62$ and 0.71 for $\gamma = 10$ and 100, respectively.

The site-occupancy profiles are plotted with respect to this alternative coordinate in Fig. 3. The greatly improved convergence lends support to the alternate method of rescaling the coordinate at finite γ. As yet, there is no theoretical explanation of this observation that departures from asymptotic behavior manifest themselves primarily as corrections to coordinate rescaling.

Similar inferences are drawn from comparison of interface number-density profiles plotted in Figs. 4 and 5 with respect to uncorrected and corrected coordinates, respectively. Again, convergence to the continuum analog, in this case $2u(1-u)$, is more rapid in the corrected coordinate.

Figures 4 and 5 raise a new question, because simple considerations would appear to rule out interface number-density values above 1/2.

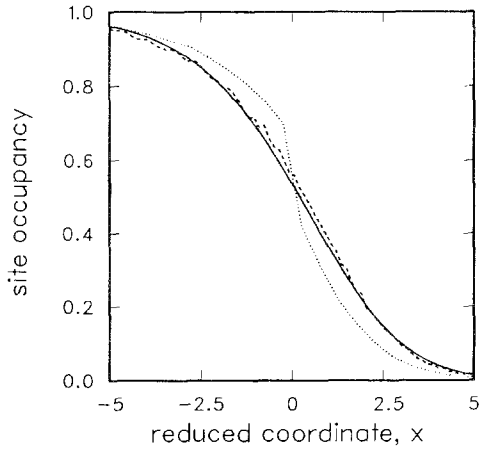

Fig. 3. Site occupancy versus reduced coordinate $x = j/(\hat{v}\sqrt{\gamma})$ for $(\cdots)$ $\gamma = 10$, $\hat{v} = 0.62$ and $(--)$ $\gamma = 100$, $\hat{v} = 0.71$ ($\hat{v}$ corrects for the lack of convergence to the asymptotic propagation velocity.) (——) The continuum profile u.

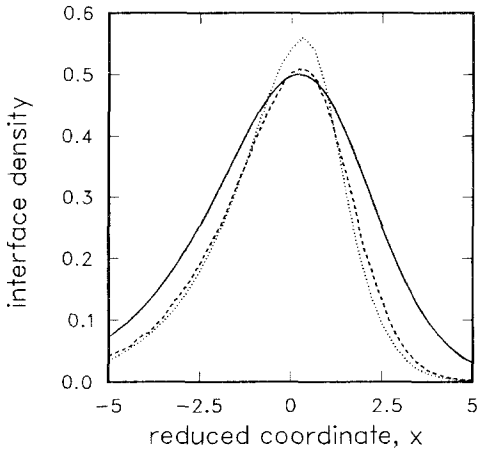

Fig. 4. Interface number density versus reduced coordinate $x = j/\sqrt{\gamma}$ for $(\cdots)$ $\gamma = 10$ and $(--)$ $\gamma = 100$. (——) The continuum profile $2u(1-u)$.

Namely, a statistically independent distribution of occupied sites at a location with occupancy u would give an interface density $2u(1-u)$, which never exceeds 1/2. Complete statistical independence is achieved only in the limit $\gamma \to \infty$. For finite γ, the creation process would appear to introduce only positive correlations between the states of nearby sites, thereby lowering the interface number density.

The explanation for computed densities exceeding 1/2 is that the origin of coordinates has been chosen at the instantaneous center of propagation,

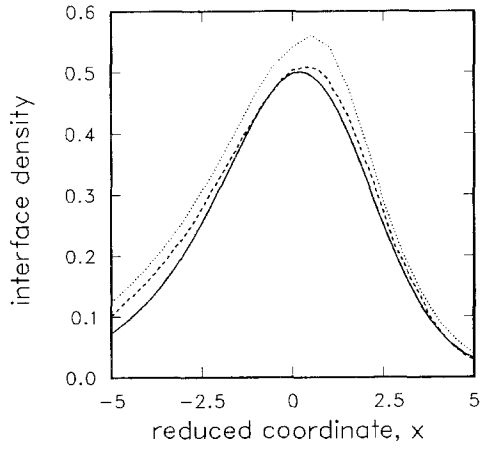

Fig. 5. Interface number density versus reduced coordinate $x = j/(\hat{v}\sqrt{\gamma})$ for $(\cdots)$ $\gamma = 10$, $\hat{v} = 0.62$ and $(--)$ $\gamma = 100$, $\hat{v} = 0.71$. (——) The continuum profile $2u(1-u)$.

a quantity that fluctuates about the ensemble-averaged center of propagation, $\bar{c} = vt$. The location of the instantaneous center may be positively correlated with local fluctuations in the interface number density, thereby allowing the computed quantity to exceed 1/2. As evidence that this may occur, consider the interface number-density profile for $\gamma = 0$. In this case, the site-occupancy profile is always a step function, with a single interface located at $j = 0$. Therefore the interface number density is unity at $j = 0$ and zero elsewhere. As γ increases, it is reasonable to expect that the interface number density at $j = 0$ decreases monotonically, approaching 1/2 in the large-γ limit. As yet, there is no analytical confirmation of this conjecture.

In summary, the computational results are consistent with analytical results derived for the hydrodynamic limit, although the computations indicate a slow rate of convergence to that limit. The computations suggest additional features of the lattice-gas model that may be of theoretical interest. These features may also prove to be of physical interest in the context of the combustion application that motivated the model.

ACKNOWLEDGMENTS

The author would like to thank J. L. Lebowitz for stimulating discussions and encouragement. This research was supported by the Division of Engineering and Geosciences, Office of Basic Energy Sciences, U. S. Department of Energy.

REFERENCES

1. A. De Masi, P. A. Ferrari, and J. L. Lebowitz, Rigorous derivation of reaction-diffusion equations with fluctuations, *Phys. Rev. Lett.* **55**:1947 (1985).
2. A. R. Kerstein, Pair-exchange model of turbulent premixed flame propagation, 21st International Symposium on Combustion, Combustion Institute, Pittsburgh (1986), in press.
3. M. Bramson, P. Calderoni, A. De Masi, P. A. Ferrari, J. L. Lebowitz, and R. H. Schonmann, Microscopic selection principle for diffusion-reaction equation, *J. Stat. Phys.*, this issue, preceding paper.
4. A. N. Kolmogoroff, I. G. Petrovsky, and N. S. Piscounoff, Études de l'équations de la diffusion avec croissance de la quantité de matière et son application a un problème biologique, *Bull. Univ. Mosc. Ser. Int. A* **1**(6):1 (1937).
5. D. G. Aronson and H. F. Weinberger, Nonlinear diffusion in population genetics, combustion and nerve pulse propagation, in *Partial Differential Equations and Related Topics*, J. Goldstein, ed. (Lecture Notes in Mathematics, No. 446, Springer, New York, 1975).
6. H. Tennekes and J. L. Lumley, *A First Course in Turbulence* (MIT Press, Cambridge, Massachusetts, 1972).
7. J. L. Lebowitz, private communication.
8. R. A. Fisher, The wave of advance of advantageous genes, *Ann. Eugenics* 7:355 (1937).